Resonator mode in chains of silver spheres and its possible application

C. R. Simovski
Physics Department, St. Petersburg University of Information Technologies, Mechanics and Optics, Sablinskaya 14, 197101, St. Petersburg, Russia and Radio Laboratory/SMARAD, Helsinki University of Technology, FI-02015 TKK, Finland

A. J. Viitanen
Electromagnetics Laboratory, Helsinki University of Technology, FI-02015 TKK, Finland

S. A. Tretyakov
Radio Laboratory/SMARAD, Helsinki University of Technology, FI-02015 TKK, Finland
(Received 18 July 2005; published 13 December 2005)

A transversal mode with zero group velocity and nonzero phase velocity that can exist in chains of silver nanospheres in the optical frequency range is theoretically studied. It is shown that the external source radiating a narrow-band nonmonochromatic signal can excite in the chain a mixture of standing and slowly traveling waves. The standing-wave component (named the resonator mode) is strongly dominating. The physical reason for such a regime is a sign-varying distribution of power flux over the cross section of the chain. A possible application of the resonator mode for evanescent-wave enhancement and for subwavelength imaging in the visible is discussed.

DOI: 10.1103/PhysRevE.72.066606 PACS number(s): 42.70.Qs, 41.20.Jb, 77.84.Lf, 73.20.Mf

I. INTRODUCTION

Recently, new imaging systems capable of resolving subwavelength details were proposed. Realization of the "perfect lens" proposed by Pendry [1] requires a realization of a low-loss artificial material with effective negative permittivity and permeability. This task is a great challenge, especially if operation in the visible is a requirement. Although in recent literature there have been reports on progress towards this goal, other possibilities to realize superresolution imaging devices should be considered. Of particular interest can be a possibility to use arrays of small resonant particles [2], which allows one to enhance evanescent fields and form subwavelength images without any bulk metamaterial. The key feature of such a particle array is that it can support slow surface waves with large wave numbers. For "ideal" operation, waves with all wave numbers that are larger than the free-space wave number should be in the eigenmode spectrum of the array. It is clear that the ideal operation is hardly realizable, but it is possible to find structures with rather "flat" regions on their dispersion curves. Specifically, one would need to have a possibility of resonant excitation of surface waves with a wide interval of wave numbers at a certain working frequency.

For optical applications, a natural choice of small resonant particles is the plasmonic nanosphere. Recent results from the literature indeed indicate a possibility to realize regimes needed for devices enhancing evanescent modes: In a recent paper by Weber and Ford [3] an interesting result was obtained for a chain of silver nanospheres operating at frequencies near the plasmon resonance of an individual sphere. Namely, if the spheres are small enough, polarized transversally with respect to the chain axis, and the chain is dense (the ratio of the sphere diameter d to the array period a is larger than 0.5), there appears a frequency band in which two propagation constants q_1 and q_2 correspond to every frequency ω. One propagation constant q_1 corresponds to a forward wave; another $q_2 > q_1$ corresponds to a backward wave. At the upper bound of this frequency band (frequency ω_r) both these solutions join one another: $q_b = q_f = q_r$. At this frequency the group velocity is zero and the phase velocity is nonzero. In the vicinity of this frequency the dispersion curve is rather flat, and there is a more or less wide range of wave numbers that can be resonantly excited by external evanescent fields.

Let us note that this zero-group-velocity regime is not the Bragg mode since it occurs not at the edge of the first Brillouin zone; see Fig. 1. The crucial difference with the Bragg mode is that the phase velocity is not equal to π/a, and therefore the wave with wave number $k_x = q_r$ and frequency ω_r does not experience the total reflection by the chain. Meanwhile, the Bragg mode of an infinite periodic structure is not supported by the chain and corresponds to the excitation of some few elements of the chain (closest to the source) and the mode under study can be excited by a source in a rather long part of the chain. The length is restricted only by losses.

In this paper we theoretically study the excitation of waves in dense chains of plasmonic nanoparticles in view of potential applications for subwavelength imaging in the optical region.

II. ZERO GROUP VELOCITY IN CHAINS OF PLASMON PARTICLES

A dispersion curve exhibiting the zero-group-velocity regime was obtained in [3] by numerical simulation of a finite chain of silver spheres with diameter $d = 50$ nm, period $a = 75$ nm (in free space). We reproduced it in [4] using an analytical solution of the explicit dispersion equation for the infinite chain of resonant dipoles. Let us briefly present our

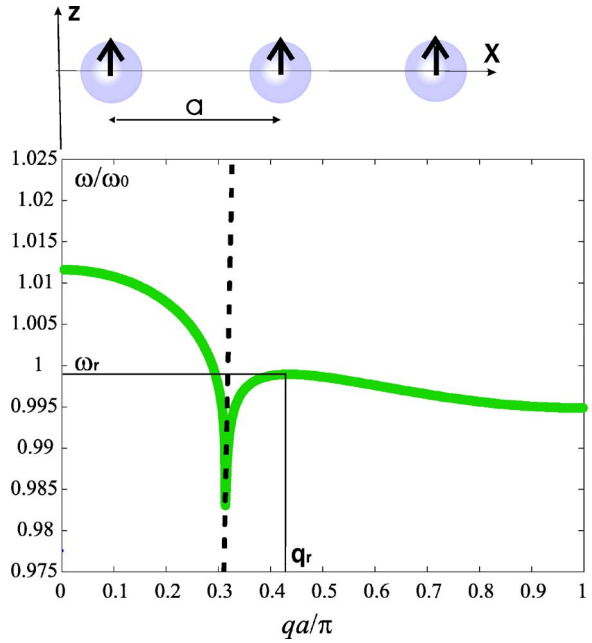

FIG. 1. (Color online) Dispersion diagram of the chain $d=50$ nm, $a=75$ nm, and $\lambda_p=272$ nm, corresponding to Fig. 3 of Ref. [3].

analytical model (note that a similar model was presented in Ref. [5], which appeared very recently). A transversally (z-)polarized sphere centered at a certain point of the axis x—e.g., at $x=0$—is chosen as a reference sphere and the z-directed dipole moment p is attributed to it. All other spheres are modeled as z-directed dipoles p_n whose phase shift with respect to the reference one is determined by the propagation constant q: $p_n=p\exp(-jqna)$. Temporal dependence is chosen as $\exp(j\omega t)$.

Neglecting losses in order to obtain a real-value dispersion equation we can write the permittivity of silver in the optical range in the form

$$\varepsilon_s = 1 - \frac{\omega_p^2}{\omega^2}, \tag{1}$$

where the plasma frequency ω_p can correspond to the wavelength 150–300 nm [6] depending on the sphere radius. Next, we write the inverse polarizability of the sphere in the form following from formulas (4) and (6) of [3]:

$$\frac{1}{\alpha} = \frac{\varepsilon_s + 2\varepsilon}{3\varepsilon_0 \varepsilon V(\varepsilon_s - \varepsilon)} + j\frac{k^3}{6\pi\varepsilon_0\varepsilon}. \tag{2}$$

Here $V=\pi d^3/6$ is the sphere volume and ε is the matrix permittivity. The difference between Eq. (2) and formula (6) of [3] is due to the Gaussian system of units adopted in [3]. The polarizability α relates the dipole moment p of the reference sphere with local field $E^{(\mathrm{loc})}$ (more exactly, its z component) which is produced by all the other dipoles. The local field can be expressed through p in terms of the interaction constant C of the dipole array:

$$E^{(\mathrm{loc})} = C(k,q,a)p, \quad p = \alpha E^{(\mathrm{loc})}. \tag{3}$$

C depends on the frequency ω (or matrix wave number $k=\omega\sqrt{\mu_0\varepsilon_0\varepsilon}$), on the propagation constant q, and on the array period a. The interaction constant of the chain of transversally polarized dipoles in a homogeneous matrix with relative permittivity ε was analytically obtained in [4] for the domain outside the light cone—i.e., within the band $k<q<2\pi/a-k$. The expression is as follows:

$$C = \frac{jk^3}{6\pi\varepsilon\varepsilon_0} - \frac{k^2}{4a\pi\varepsilon\varepsilon_0}\ln(2|\cos qa - \cos ka|) - \frac{1}{2\pi\varepsilon\varepsilon_0}\sum_{n=1}^{+\infty}\left[\frac{k\sin nka}{(na)^2} + \frac{\cos nka}{(na)^3}\right]\cos nqa. \tag{4}$$

The logarithmic term describes the wave interaction of dipoles. For lossless particles the dispersion equation $1/\alpha=C$ transits to the real equation

$$\mathrm{Re}\left(\frac{1}{\alpha}\right) = \mathrm{Re}(C), \tag{5}$$

since the imaginary parts of the interaction constant and that of the inverse polarizability cancel out.

The solution of the dispersion equation (5) for the same parameters as in [3] ($a=1.5d=75$ nm, $\lambda_p=272$ nm, $\varepsilon=1$) allows us to reproduce with a high accuracy the numerical results of [3]. The curve shown in Fig. 1 visually coincides with the dispersion plot shown in Fig. 3 of [3]. The guided mode wave number q becomes really different from the free-space one k only near the plasmon resonance of a sphere $\omega=\omega_0$ (in our case it corresponds to $ka=1$). The zero group velocity corresponds to $\omega_r=0.999\omega_0$ and $q_r=0.411\pi/a$ (we call it a *resonator mode*). Within the very narrow band of normalized frequencies $0.998<\omega/\omega_0<0.999$ the rather large interval of propagation constants lies $0.36\pi<qa<0.6\pi$.

In [3] it was shown that the eigenmode for a system of 20 z-polarized spheres almost coincides with that for infinite chain (Fig. 1). So both backward and forward modes should exist in a finite chain within the frequency range under consideration. Even the presence of losses in silver (these losses were also simulated in the cited work) does not practically disturb the dispersion curve shown in Fig. 1 (the curve for lossy silver is also shown in Fig. 3 of [3]). The very important questions are as follows: How to excite the mode at the frequency ω_r and what happens in the chain with the pulse occupying a narrow but finite range $\omega_1,\ldots,\omega_r$?

Notice that an exotic mode with zero group velocity and nonzero phase velocity is not a new phenomenon. Probably, the first known structure with this property is a surface wave on an interface between two media, such that one of the media has normal dispersion, but the other has anomalous dispersion. This case was considered in [7] in connection with waves having complex amplitudes. At a special frequency the surface wave stops propagating and the total power flux equals zero, though in two media separately the Poynting vectors are nonzero. Another publication revealing a similar regime was [8]. In that work the authors studied

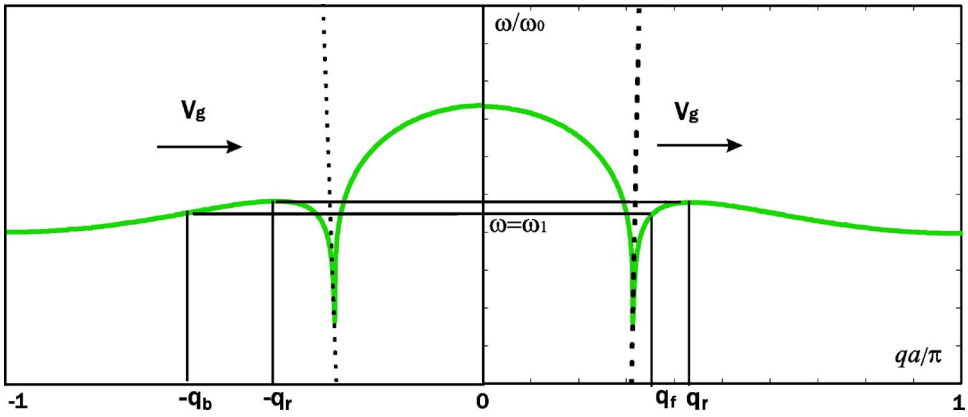

FIG. 2. (Color online) Two waves, a forward one and backward one, both with positive group velocity ($V_g>0$), are excited in the right part of the chain (with respect to the source) at the frequency $\omega_1 \approx \omega_r$. At the frequency ω_r both q_f and q_b transit to q_r and $V_g \to 0$.

hybrid waves in a microwave parallel-plate waveguide containing a ferrite layer with tangential magnetization which was located between two dielectric layers (for example, two air spacings). At the special frequency corresponding to zero group velocity of the eigenmode the wave was forward in the two dielectric layers and backward in the ferrite layer, so that the averaged total power flux was zero. A similar situation happens in coupled waveguides—e.g., in coupled periodically loaded rectangular waveguides (also considered in [7]) and in waveguides formed by channels in photonic crystals (e.g., [11]). One can obtain the so-called odd excitation of these guides when the forward wave propagating in the first channel excites the backward wave with the same amplitude in the second one. For the waveguides in photonic crystal this can happen for real-value wave numbers of guided modes [11]. A new pulse to study such systems is related to composite materials exhibiting both negative permittivity and negative permeability in the same frequency range. This property corresponds to the negative refraction index of a medium. Waves with zero group velocity and nonzero phase one in the negative refraction-index waveguides were studied in Refs. [9,10]. The vortex character of the Poynting vector distribution was shown in these works as well as the absence of the fundamental mode in this regime. The effect of the zero group velocity with a nonzero phase one was also obtained (though not discussed) in papers devoted to microstrip lines with negative refraction and to electromagnetic band-gap surfaces (artificial periodic structures with resonant surface impedance) [12,13]. The present paper develops the topic concerning such an exotic mode for chains of nanoparticles, emphasizing the problems of their excitation and propagation of a light pulse in such chains. The spatial distribution of the Poynting vector of the mode is also studied.

III. EXCITATION OF THE CHAIN BY A LINE SOURCE

Let a z-polarized line source stretched along OY with dipole moment per unit length (p.u.l.) $\mathcal{P}_s$ be located at the point $x=x_0$, $z=0$ where $x_0 \to -\infty$. This geometry of the excitation allows us to ignore the interaction of the reference sphere centered at the point $x=0$ with the particles positioned near the source.

Let $f(k,x,z)$ denote any component of the field produced by the source radiating at the frequency $\omega=k/\sqrt{\mu_0\varepsilon_0\varepsilon}$. We expand $f(k,x,z)$ into a spatial spectrum defined as

$$f(k,k_x,z) \equiv \int_{-\infty}^{\infty} f(k,x,z)e^{jk_x x}dx. \tag{6}$$

The external field exciting the chain of spheres contains harmonics with $k_x>k$ and $k_x<-k$, which are evanescent with respect to z and propagating along x within the interval $-\infty<x<\infty$ in both positive and negative directions and the spatial spectrum, is symmetric—i.e., $f(k_x)=f(-k_x)$.

The Fourier transform allows us to single out the resonant contribution of harmonics $k_x=q$ (where q is a solution of the dispersion equation) into induced polarization of the chain. This resonant contribution is due to the phase synchronism of a spatial harmonic of the external field with $k_x=q$ and an eigenmode of the chain. The eigenmodes are excited by evanescent waves (with respect to the z axis) having $|k_x|>k$. If the source oscillates at the frequency $\omega_1 \approx \omega_r$ so that $\omega_1<\omega_r$ (as shown in Fig. 2), two waves will be excited in an infinite lossless chain within the interval $x>x_0$: a forward wave with wave vector $k_x=q_f$ and a backward wave with wave vector $k_x=-q_b$. This happens because the source is positioned on the left from the considered spatial domain, so that the group velocity of both excited eigenwaves should be directed to the right, away from the source. This means that for the backward wave we should choose the negative dispersion branch with $k_x=-q_b$; see Fig. 2.

We will use the Floquet expansion for the chain polarization. For the polarization per unit length of the chain we can write

$$\mathcal{P}(x) = \mathcal{P}_f + \mathcal{P}_b = aA_f \sum_{m=-\infty}^{\infty} \delta(x-ma)e^{-jq_f x} + aA_b \sum_{m=-\infty}^{\infty} \delta(x-ma)e^{jq_b x}. \tag{7}$$

In this equation A_f and A_b are unknown values related to the spatial spectrum of the external field $f(k_x)$. Using the Poisson summation formula we obtain the Floquet expansion for polarization p.u.l.:

$$\mathcal{P}_f(x) + \mathcal{P}_b(x) = A_f \sum_{m=-\infty}^{\infty} e^{-j(q_f + 2\pi m/a)x} + A_b \sum_{m=-\infty}^{\infty} e^{j(q_b - 2\pi m/a)x}. \tag{8}$$

Let us find A_f and A_b. The crucial factor of the theory is the relation between A_f and A_b that determines the contribution of the standing wave in the excited field. In this section we will obtain the result $A_f \approx A_b$, and below we will show that the standing wave is dominating.

The vector potential of the external field within the interval $-\infty < x < \infty$ is equal to

$$\mathbf{A}_s(x,z) = \frac{\omega\mu_0 \mathcal{P}_s}{4} H_0^{(2)}[k\sqrt{(x-x_0)^2 + z^2}]\mathbf{z}_0 \tag{9}$$

[where $H_0^{(2)}$ denotes Hankel's function of the second kind] and its Fourier transform is as follows:

$$\mathbf{A}_s(k_x,z) = \frac{-j\omega\mu_0 \mathcal{P}_s}{2\sqrt{k^2 - k_x^2}} e^{-jk_x x_0} e^{-j\sqrt{k^2 - k_x^2}|z|}\mathbf{z}_0. \tag{10}$$

Using the Lorentz gauge we easily obtain the Fourier transform of the z component of $\mathbf{E}_s$ at the plane $z=0$:

$$E_{zs}(k_x,0) = \frac{k_x^2 \mathcal{P}_s e^{jk_x x_0}}{2\varepsilon\varepsilon_0\sqrt{k^2 - k_x^2}} = \frac{k_x^2 \mathcal{P}_s e^{-jk_x|x_0|}}{2\varepsilon\varepsilon_0\sqrt{k^2 - k_x^2}}. \tag{11}$$

Every spatial harmonic $E_{zs}(k_x,0)\exp(-jk_x x)$ induces a periodic distribution of dipole moments along the chain $p_n(k_x) = p(k_x)\exp(-jk_x na)$, and from Eq. (3) we obtain the following equation for the reference dipole moment excited by this spatial harmonic:

$$\frac{1}{\alpha} p(k_x) = E_z(k_x,0) + C(k_x)p(k_x). \tag{12}$$

Here the first term on the right-hand side is the spatial harmonic of the external field taken at $x=0$ and the second term is the corresponding interaction field of the chain. With Eqs. (11) and (12) the reference dipole moment excited at the given frequency reads as

$$p = \int_{-\infty}^{\infty} \frac{k_x^2 \mathcal{P}_s}{4\pi\varepsilon\epsilon_0\sqrt{k^2 - k_x^2}} \frac{e^{-jk_x|x_0|}}{\mathrm{Re}\left(\frac{1}{\alpha}\right) - \mathrm{Re}[C(k_x)]} dk_x. \tag{13}$$

Following the principle illustrated by Fig. 2 we can attribute to the roots of the dispersion equation $k_x = q_f$ and $k_x = -q_b$ infinitesimally small negative imaginary parts. Indeed, these waves transport energy from the source and therefore must attenuate along x. Then in the lower half-plane of the complex variable k_x the integrand in Eq. (13) has two poles $k_x = q_f$ and $k_x = -q_b$. The contribution of these poles is residual:

$$p = \pi\mathcal{P}_s\left(\frac{q_f^2 e^{-jq_f|x_0|}}{\sqrt{q_f^2 - k^2}\Phi(q_f)} + \frac{q_b^2 e^{jq_b|x_0|}}{\sqrt{q_b^2 - k^2}\Phi(-q_b)}\right), \tag{14}$$

where we have denoted

$$\Phi(q) = 4\pi\varepsilon\varepsilon_0 \frac{d}{dq}\left[\mathrm{Re}\left(\frac{1}{\alpha}\right) - \mathrm{Re}[C(q)]\right] = -4\pi\varepsilon\varepsilon_0 \frac{d\,\mathrm{Re}[C(q)]}{dq}.$$

In Eq. (14) we have neglected the contribution of the branch cut around $k_x = k$ (which describes the cylindrical wave field attenuating from the source). The results for A_f and A_b follow from Eq. (14) and definition (7):

$$A_{f,b} = \pm\pi\mathcal{P}_s e^{\mp jq_{f,b}|x_0|} \frac{q_{f,b}^2}{\sqrt{(q_{f,b}a)^2 - (ka)^2}|\Phi(q_{f,b})|}. \tag{15}$$

In Eq. (15) the minus sign for $q = q_b$ takes into account that $\Phi(q)$ is an odd function of q. From Eq. (15) the following relations can be derived:

$$A_f = A_0(q_f)e^{-jq_f|x_0|}, \quad A_b = -A_0(q_b)e^{jq_b|x_0|}. \tag{16}$$

Here

$$A_0(q) = q^2\mathcal{P}_s\pi\sqrt{(qa)^2 - (ka)^2}|\Phi(q)| \tag{17}$$

is a slowly varying function.

Let us show that the relation $A_0(q_f) = A_0(q_b)$ holds with a high accuracy for $\omega \approx \omega_r$. From Eq. (4) we easily obtain

$$\Phi(q) = \frac{1}{a^2}\left[\frac{(ka)^2 \sin qa}{(\cos ka - \cos qa)} + 2\sum_{n=1}^{+\infty} \frac{\cos nka \sin nqa}{(n)^2} + 2ka\frac{\sin nka \sin nqa}{n}\right].$$

Using the tabulated series

$$\sum_{m=1}^{+\infty} \frac{e^{-j\gamma m}}{m} = -\ln(1 - e^{-j\gamma}) = -\left(\ln\left|2\sin\frac{|\gamma|}{2}\right| + j\frac{\pi - \gamma'}{2}\right), \tag{18}$$

where $\gamma' = 2\pi\{\gamma/(2\pi)\}$ and the notation $\{x\}$ is used for fractional part of variable x, we obtain, for $\Phi(q)$,

$$\Phi(q) = \frac{1}{a^2}\left[\frac{(ka)^2 \sin qa}{(\cos ka - \cos qa)} + 2\sum_{n=1}^{+\infty} \frac{\cos nka \sin nqa}{(n)^2} + ka \ln\left|\frac{\sin\left(\frac{qa + ka}{2}\right)}{\sin\left(\frac{qa - ka}{2}\right)}\right|\right]. \tag{19}$$

Formula (19) should be substituted into Eq. (17). At the frequency $\omega = 0.998\omega_0$ from the dispersion curve shown in Fig. 1 we have $q_f a = 0.401\pi = 0.957 q_r a$ and $q_b a = 0.440\pi = 1.050 q_r a$. Substituting these values into Eqs. (15) and (19) we obtain $A_b/A_f \approx -0.945\exp(j2.007 q_r|x_0|)$. Thus, when $\omega \approx \omega_r$ the relation $|A_b| \approx |A_f|$ indeed holds.

Relation (16) for $\omega \approx \omega_r$ can be approximately rewritten as

$$\frac{A_b}{A_f} \approx -e^{j(q_b+q_r)|x_0|}. \tag{20}$$

Let us show that the ratio (20) practically does not depend on the frequency in the vicinity of the point ω_r. At ω_r the function $q(\omega)$ has zero derivative, and since the dispersion curve is smooth, we can approximate it as

$$q(\omega) = q_r + \alpha(\omega_r - \omega)^2. \tag{21}$$

Here α is a finite coefficient. Then $q_b = q_r + \Delta q(\omega)$ and $q_f = q_r - \Delta q(\omega)$, where we denoted $\Delta q(\omega) = \alpha(\omega_r - \omega)^2$. So we can rewrite Eq. (20) as

$$\frac{A_b}{A_f} \approx -e^{2jq_r|x_0|}. \tag{22}$$

Thus, the two propagating modes $-q_b$ and q_f are excited with practically the same efficiency when $\omega \approx \omega_r$. Note that the phase shift between A_f and A_b is not the real phase shift between the forward and backward waves excited in the chain. Recall that $A_{f,b}$ are components of the dipole moment of the reference sphere which is distanced by $|x_0|$ from the source. It is physically sound that the ratio A_b/A_f depends on x_0.

IV. POYNTING VECTOR EVALUATION

In this section we study the spatial distribution of the axial component of the Poynting vector in the excited chain. The purpose is to understand the energetic mechanism of the standing wave excitation in the infinite chain.

The field produced by every term (Floquet's harmonic) of Eq. (8) is known: This is the field of a continuous transversal polarization with harmonic dependence along the axis. Let us denote $\rho = \sqrt{y^2+z^2}$ and let k_{xm} denote either $k_{xm} = q_f + 2\pi m/a$ or $k_{xm} = -q_b + 2\pi m/a$. In polar coordinates (ρ, z, φ) all the components of the field produced by every Floquet's harmonic of $\mathcal{P}(x)$ can be written using formulas (5.32) of [15]:

$$E_{\rho m} = \frac{A}{j4\epsilon_0}\cos\varphi\left[(k^2 - k_{xm}^2)\frac{H_1^{(2)}(\sqrt{k^2-k_{xm}^2}\rho)}{\sqrt{k^2-k_{xm}^2}\rho} + k_{xm}^2 H_0^{(2)}(\sqrt{k^2-k_{xm}^2}\rho)\right]e^{-jk_{xm}x}, \tag{23}$$

$$E_{\varphi m} = \frac{A}{j4\epsilon_0}\sin\varphi\left[(k^2 - k_{xm}^2)\frac{H_1^{(2)}(\sqrt{k^2-k_{xm}^2}\rho)}{\sqrt{k^2-k_{xm}^2}\rho} - k^2 H_0^{(2)}(\sqrt{k^2-k_{xm}^2}\rho)\right]e^{-jk_{xm}x}, \tag{24}$$

$$E_{xm} = \frac{A}{4\epsilon_0 a}\cos\varphi k_{xm}\sqrt{k^2-k_{xm}^2}H_1^{(2)}(\sqrt{k^2-k_{xm}^2}\rho)e^{-jk_{xm}x}, \tag{25}$$

$$H_{\rho m} = -\frac{j\omega A}{4}k_{xm}\sin\varphi H_0^{(2)}(\sqrt{k^2-k_{xm}^2}\rho)e^{-jk_{xm}x}, \tag{26}$$

$$H_{\varphi m} = -\frac{j\omega A}{4}k_{xm}\cos\varphi H_0^{(2)}(\sqrt{k^2-k_{xm}^2}\rho)e^{-jk_{xm}x}, \tag{27}$$

$$H_{xm} = \frac{\omega A}{4a}\sin\varphi\sqrt{k^2-k_{xm}^2}H_1^{(2)}(\sqrt{k^2-k_{xm}^2}\rho)e^{-jk_{xm}x}. \tag{28}$$

Here $A = A_b$ for the fields of the backward wave and $A = A_f$ for the fields of the forward wave. The total field produced by the chain is the sum

$$\mathbf{E}^t = \mathbf{E}^f + \mathbf{E}^b, \quad \mathbf{H}^t = \mathbf{H}^f + \mathbf{H}^b, \tag{29}$$

where the index t denotes the total field and the field of the source is neglected ($|x_0| \to \infty$). In this way both forward-wave and backward-wave components of the field produced by the chain are represented as Floquet's series of terms (23)–(28) [all the coefficients in these expansions equal unity in accordance with Eq. (8)].

The Poynting vector is proportional to the vector product of the total electric and magnetic fields. The axial component of the Poynting vector responsible for the energy transport is as follows:

$$S_x^t = \frac{1}{2}\,\mathrm{Re}\{(E_\rho^t H_\varphi^{t*} - E_\varphi^t H_\rho^{t*})\}. \tag{30}$$

Representing the total field as the sum of harmonics (23)–(28) we obtain that the Poynting vector splits into four terms,

$$S_x^t = S^{ff} + S^{bb} + S^{fb} + S^{bf}, \tag{31}$$

where for every term of Eq. (31) the following expansion is obtained:

$$S^{\alpha\beta} = \sum_{m=-\infty}^{\infty}\sum_{n=-\infty}^{\infty} S_{mn}^{\alpha\beta} = \sum_{m=-\infty}^{\infty}\sum_{n=-\infty}^{\infty}\frac{1}{2}\,\mathrm{Re}\{(E_{\rho m}H_{\varphi n}^* - E_{\varphi m}H_{\rho n}^*)\}. \tag{32}$$

In this equation $E_{\rho m}$, $H_{\varphi n}$, $H_{\rho n}$, and $E_{\varphi n}$ are determined by relations (23)–(28) and

$$k_{xm} = q_f + \frac{2\pi m}{a}, \quad k_{xn} = q_f + \frac{2\pi n}{a} \quad \text{for } S^{ff}, \tag{33}$$

$$k_{xm} = -q_b + \frac{2\pi m}{a}, \quad k_{xn} = -q_b + \frac{2\pi n}{a} \quad \text{for } S^{bb}, \tag{34}$$

$$k_{xm} = q_f + \frac{2\pi m}{a}, \quad k_{xn} = -q_b + \frac{2\pi n}{a} \quad \text{for } S^{fb}, \tag{35}$$

$$k_{xm} = -q_b + \frac{2\pi m}{a}, \quad k_{xn} = q_f + \frac{2\pi n}{a} \quad \text{for } S^{bf}. \tag{36}$$

Every term $S_{mn}^{\alpha\beta}$ of the series (32) (α and β mean f or b) reads

$$S_{mn}^{\alpha\beta}(\rho,\varphi,x) = \frac{1}{2}\,\mathrm{Re}\left\{\frac{\omega A_1 A_2^* k_{xn}}{16\epsilon_0}\left[\cos^2\varphi\left((k^2-k_{xm}^2)\times\frac{H_1^{(2)}(\sqrt{k^2-k_{xm}^2}\rho)}{\sqrt{k^2-k_{xm}^2}\rho}+k_{xm}^2 H_0^{(2)}(\sqrt{k^2-k_{xm}^2}\rho)\right)\times H_0^{(2)*}(\sqrt{k^2-k_{xn}^2}\rho)-\sin^2\varphi\left((k^2-k_{xm}^2)\times\frac{H_1^{(2)}(\sqrt{k^2-k_{xm}^2}\rho)}{\sqrt{k^2-k_{xm}^2}\rho}-k^2 H_0^{(2)}(\sqrt{k^2-k_{xm}^2}\rho)\right)\times H_0^{(2)*}(\sqrt{k^2-k_{xn}^2}\rho)\right]e^{-j(k_{xm}-k_{xn})x}\right\}. \quad (37)$$

Here $A_1=A_2=A_f$ for S_{mn}^{ff}, $A_1=A_2=A_b$ for S_{mn}^{bb}, and $A_1=A_f$, $A_2=A_b$ for $S_{mn}^{fb,bf}$.

Relation (37) describes the axial Poynting vector as the function of all three polar coordinates. To check ourselves we have considered the radial component of the Poynting vector and proved the power balance in the leaky regime. We have shown that in both waveguide and leaky regimes the Poynting vector distribution is vortex since $\nabla\times\mathbf{S}\neq\mathbf{0}$ on the axis x (this result was also obtained in [8] for a layered waveguide with the opposite energy flow directions in the layers).

Here we concentrate on the averaged power flux along the chain. This flux corresponds to averaging of S_x^t over both azimuthal angle φ and coordinate x. The integration with respect to angle φ gives π in each term of Eq. (37), and the terms with $H_1^{(2)}(\sqrt{k^2-k_{xm}^2}\rho)$ cancel out. Further, averaging over x leaves only the terms with $m=n$ due to the factor $\cos(k_{xm}-k_{xn})x$. Moreover, after averaging over x the terms S^{bf} and S^{fb} cancel out, because due to the difference between q_b and q_r, the diagonal terms $S_{mm}^{bf,fb}$ are proportional to $\cos(q_b-q_f)x$.

Because $q>k$, the argument of Hankel's functions in Eq. (37) is imaginary. Since $H_0^{(2)}(-jz)=(j2/\pi)K_0(z)$, where $K_0(z)$ is the real-valued McDonald's function, the averaged over x and φ axial component of the Poynting vector reads

$$\langle S_x^t(\rho)\rangle = \sum_{m=-\infty}^{\infty}(\langle S_{mm}^{ff}\rangle+\langle S_{mm}^{bb}\rangle), \quad (38)$$

$$\langle S_{mm}^{ff,bb}\rangle = \frac{\omega|A_{f,b}|^2}{8\pi\epsilon_0 a^2}k_{xm}(k_{xm}^2+k^2)K_0^2(\sqrt{k_{xm}^2-k^2}\rho). \quad (39)$$

Here for $\langle S_{mm}^{ff}\rangle$ we should substitute $k_{xm}=q_f+2\pi m/a$ and for $\langle S_{mm}^{bb}\rangle$ we should substitute $k_{xm}=-q_b+2\pi m/a$. The series (38) converges exponentially except a singular point $\rho=0$, but the singularity is integrable. The basic harmonic for $\rho\neq 0$ is dominating; the contribution of others in the series sum is marginal. Denoting

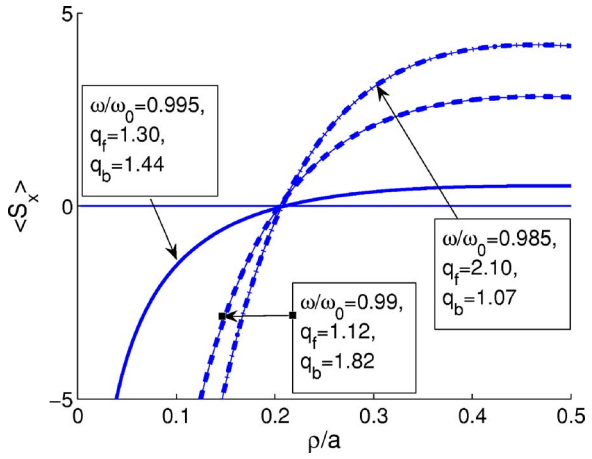

FIG. 3. (Color online) Power density distribution (in arbitrary units) in the vicinity of the chain axis when the two-mode regime is excited in the chain corresponding to Fig. 1 at three different frequencies close to ω_r. The domain $\rho>a$ where all the curves exponentially tend to zero is not shown.

$$B_{f,b} = |A_{f,b}|^2\frac{\omega}{8\pi\epsilon_0 a^2} \quad (40)$$

and neglecting the contribution of high-order Floquet harmonics we have

$$\langle S_x^t(\rho)\rangle = B_f q_f(q_f^2+k^2)K_0^2(\sqrt{q_f^2-k^2}\rho) - B_b q_b(q_b^2+k^2)K_0^2(\sqrt{q_b^2-k^2}\rho). \quad (41)$$

The power density attenuates exponentially in the radial direction when $\rho\to\infty$. When ω is close to ω_r then $|A_b|\approx|A_f|$ as we have shown above and $B_b\approx B_f$. So when $\omega\approx\omega_r$ we can rewrite Eq. (41), denoting $B_f\approx B_b=B$ in the form

$$\langle S_x^t(\rho)\rangle \approx B[q_f(q_f^2+k^2)K_0^2(\sqrt{q_f^2-k^2}\rho) - q_b(q_b^2+k^2)K_0^2(\sqrt{q_b^2-k^2}\rho)]. \quad (42)$$

In Fig. 3 we present the radial distribution of the axial Poynting vector in the vicinity of the chain axis. The coefficient in front of K_0 function is greater for the backward wave than that for the forward wave, but the backward wave attenuates faster. Therefore at a certain distance ρ_0 (which is determined by the chain period a but is much smaller than a) the axial Poynting vector changes sign. In a very narrow "tube" around the chain axis the energy propagates backward. Outside this tube it propagates forward. Practically, all the power is concentrated within a tube whose radius is close to $4\rho_0,\ldots,5\rho_0$ and is of the order a. The forward energy flux ($\rho>\rho_0$) weakly dominates:

$$P_x = \int_0^{\infty}\langle S_x^t\rangle\rho d\rho > 0. \quad (43)$$

However, the total power flux is much smaller than that of mode q_f or that of mode q_b taken separately [the first and second terms in Eq. (41)]. We can accurately show integrating every spatial harmonic of $\langle S_x^t\rangle$ in Eq. (43) that P_x is proportional to the small factor $(\omega-\omega_r)/\omega_r$. For the zeroth-

order one, substituting Eq. (42) into Eq. (43) we obtain

$$P_x = B\left[q_f(q_f^2+k^2)\int_0^\infty K_0(\sqrt{q_f^2-k^2}\rho)\rho d\rho - q_b(q_b^2+k^2)\int_0^\infty K_0^2(\sqrt{q_b^2-k^2}\rho)\rho d\rho \right] = B\left[\frac{q_f(q_f^2+k^2)}{q_f^2-k^2} - \frac{q_b(q_b^2+k^2)}{q_b^2-k^2} \right]. \quad (44)$$

Using Eq. (44) it is easy to show that, when $q_b - q_f \ll (q_b + q_f)/2$,

$$P_x \approx B\frac{(q_b-q_f)(q_a^2+k^2)^2}{(q_a^2-k^2)^2}, \quad q_a \equiv \frac{q_b+q_f}{2},$$

and consequently P_x is practically proportional to $(\omega-\omega_r)/\omega_r P_r$, where P_r is the power flux corresponding to the excitation of the harmonic q_r. The value ρ_0 is a parameter of the chain that almost does not depend on the frequency. The distribution of the averaged Poynting vector around the chain axis is shown in Fig. 3 for three different frequencies. When $\omega \to \omega_r$ the axial Poynting vector tends to zero everywhere. From Eq. (44) it is clear that the power flux vanishes at $\omega=\omega_r$ ($q_b=q_f=q_r$).

V. NARROW-BAND PULSE IN THE CHAIN

In this section we consider the electric field at the axis of the chain and prove that this field is the sum of the standing wave and the traveling wave, where the standing-wave component (resonator mode) strongly dominates.

Neglecting the higher Floquet harmonics we have, for the ρ and φ components of the modal field [see Eqs. (23) and (24)],

$$E_\rho = \frac{A}{j4\varepsilon\epsilon_0}\cos\varphi\left[(k^2-q^2)\frac{H_1^{(2)}(\sqrt{k^2-q^2}\rho)}{\sqrt{k^2-q^2}\rho} + q^2 H_0^{(2)}(\sqrt{k^2-q^2}\rho) \right] e^{-jqx},$$

$$E_\varphi = \frac{A}{j4\varepsilon\epsilon_0}\sin\varphi\left[(k^2-q^2)\frac{H_1^{(2)}(\sqrt{k^2-q^2}\rho)}{\sqrt{k^2-q^2}\rho} - k^2 H_0^{(2)}(\sqrt{k^2-q^2}\rho) \right] e^{-jqx},$$

where $A=A_f$, $q=q_f$ or $A=A_b$, $q=-q_b$. Let us define the averaged z component of the electric field as follows:

$$\langle E_z\rangle = \frac{1}{2\pi^2 R_0^2}\int_0^{2\pi} d\varphi \int_0^{R_0} \rho d\rho E_z^t. \quad (45)$$

Here R_0 is the radius of the effective cross section of the guided modes (the value of the order a). Then using the relation $E_z = E_\rho\cos\varphi - E_\varphi\sin\varphi$ we obtain, from Eq. (45),

$$\langle E_z\rangle = \frac{Ae^{-jqx}(k^2+q^2)}{4\epsilon_0\varepsilon\pi R_0^2}\int_0^{R_0}\rho d\rho K_0(\sqrt{q^2-k^2}\rho).$$

In this relation the contribution of $H_1^{(2)}(\sqrt{k^2-q^2}\rho)$ cancels out. Since McDonald's functions are rapidly vanishing versus ρ, we can write

$$\int_0^{R_0}\rho d\rho K_0(\sqrt{q^2-k^2}\rho) \approx \int_0^\infty \rho d\rho K_0(\sqrt{q^2-k^2}\rho) = \frac{1}{q^2-k^2}$$

and finally obtain

$$\langle E_z\rangle = Fe^{-jqx}, \quad F = \frac{A(k^2+q^2)}{4\epsilon_0\pi R_0^2(q^2-k^2)}. \quad (46)$$

In the second relation (46), A is the amplitude of the mode—i.e., $A=A_f$ or $A=A_b$.

At a given frequency $\omega \approx \omega_r$ both forward and backward waves are excited and we have, for the total field,

$$\langle E_z^t(\omega,x)\rangle = F_f e^{-jq_f(\omega)x} + F_b e^{jq_b(\omega)x}. \quad (47)$$

Here [see Eqs. (16), (22), and (46)]

$$F_f \approx e^{-jq_f|x_0|}\frac{A_0(q_r)(k^2+q_r^2)}{4\varepsilon\epsilon_0\pi R_0^2(q_r^2-k^2)},$$

$$F_b \approx -e^{jq_b|x_0|}\frac{A_0(q_r)(k^2+q_r^2)}{4\varepsilon\epsilon_0\pi R_0^2(q_r^2-k^2)}$$

and we can write

$$F_f \approx e^{-jq_f|x_0|}F_0, \quad F_b \approx -e^{jq_b|x_0|}F_0, \quad (48)$$

where

$$F_0 = \frac{A_0(k,q_r)(k^2+q_r^2)}{4\epsilon_0\pi R_0^2(q_r^2-k^2)}. \quad (49)$$

When $\omega=\omega_r$, then $q_f=q_b=q_r$ and we obtain from Eqs. (47) and (48) a purely standing wave:

$$\langle E_z^t(\omega_r,x)\rangle = -2jF_0(\omega_r,q_r)\sin q_r(x-x_0).$$

The amplitude of the wave does not depend on the source location, as it must. In practical cases the source can radiate a signal with a very narrow but a finite frequency band. Let us denote the bandwidth as $\Delta\omega=\omega_r-\omega_2$, where ω_2 is the lower bound of the band, and show that the field $\langle E_z^t(t,x)\rangle$ is a mixture of standing and traveling waves.

The temporal dependence of the source polarization $\mathcal{P}_s(t)$ determines $F_0(\omega,q_r)$, as follows from Eqs. (17) and (49). We denote the inverse Fourier transform of the function $F_0(\omega,q_r)$ as

$$F_0(t) = \int_{\omega_2}^{\omega_r} F_0(\omega,q_r)e^{j\omega t}d\omega. \quad (50)$$

Now we can evaluate $\langle E_z^t(t,x)\rangle$ using Eq. (47):

$$\langle E_z(t,x)\rangle = \int_{\omega_2}^{\omega_r} e^{j\omega t} F_0(\omega,q_r)(e^{-jq_f(\omega)(x-x_0)} - e^{jq_b(\omega)(x-x_0)})d\omega. \tag{51}$$

Since $q_b(\omega)=q_r+\Delta q(\omega)$ and $q_f(\omega)=q_r-\Delta q(\omega)$, relation (51) can be rewritten as

$$\langle E_z(t,x)\rangle = -2j \sin q_r(x-x_0)$$

$$\int_{\omega_2}^{\omega_r} e^{j\omega t - j\Delta q(\omega)(x-x_0)} F_0(\omega,q_r)d\omega. \tag{52}$$

Since $\Delta q(\omega)=\alpha(\omega-\omega_r)^2$, expanding the exponential $\exp[-j\Delta q(\omega)(x-x_0)]$ into a Taylor series, we obtain

$$\langle E_z(t,x)\rangle = -2j \sin q_r(x-x_0)\sum_{n=0}^{\infty} \frac{[-j\alpha(x-x_0)]^n}{n!}$$

$$\int_{\omega_2}^{\omega_r} (\omega-\omega_r)^{2n} F_0(\omega,q_r)e^{j\omega t}d\omega. \tag{53}$$

Using the relations

$$(\omega-\omega_r)^{2n} = \sum_{m=0}^{2n} A_m^{(2n)}\omega^m$$

and

$$\int_{\omega_2}^{\omega_r} \omega^m F_0(\omega,q_r)e^{j\omega t}d\omega = \frac{d^m F_0(t)}{dt^m},$$

we can rewrite Eq. (53) as a series

$$\langle E_z(t,x)\rangle = -2j \sin q_r(x-x_0)\sum_{n=0}^{\infty}$$

$$\sum_{m=0}^{2n} A_m^{(2n)}\frac{[-j\alpha(x-x_0)]^n}{n!}\frac{d^m F_0(t)}{dt^m}. \tag{54}$$

Since the radiated pulse is a very narrow band, we have

$$\left|\frac{d^m \mathcal{P}_s(t)}{dt^m}\right| \ll \omega_r^m |\mathcal{P}_s(t)|$$

and consequently [see Eqs. (17) and (49)]

$$\left|\frac{d^m F_0(t)}{dt^m}\right| \ll \omega_r^m |F_0(t)|.$$

Neglecting in Eq. (54) all the terms with temporal derivatives of $F_0(t)$ and taking into account that $A_0^{(2n)}=\omega_r^{2n}$, we come to an expression for a standing wave:

$$\langle E_z(t,x)\rangle \approx -2j \sin q_r(x-x_0)F_0(t)e^{-j\alpha\omega_r^2(x-x_0)}. \tag{55}$$

The traveling-wave component is related to the inaccuracy of Eq. (55)—i.e., the series of the neglected terms containing $d^m F_0(t)/dt^m$ with $m\neq 0$. It is possible to evaluate it numerically for an explicit temporal dependence $\mathcal{P}_s(t)$ using Eqs. (17), (49), and (52); however, such estimations are not the purpose of the present paper. We only claim the presence of the standing wave in the infinite chain excited by a finite source. The smallness of the traveling-wave component follows from the results of the preceding section.

It is clear that the function $F_0(t)$ given by Eqs. (17), (49), and (50) represents the temporal dependence of the pulse distorted by the dispersion in the chain. The pulse field splits into two additive parts: a standing-wave part (resonator mode) and a traveling-wave part. The traveling-wave part has a smaller amplitude than the standing wave, and this result corresponds to the small energy flux obtained above. One can represent this small positive power flux as a sum of two parts. One part (negative) is equal to the integral over the domain $\rho<\rho_0$ in Eq. (43). The other part, positive, is equal to the integral over the domain $\rho>\rho_0$.

The effective group velocity of the pulse with frequency range $\Delta\omega$ is approximately equal to $\Delta\omega$ divided by the interval of the wave numbers of the pulse (see also Fig. 2):

$$V_g \approx \frac{\Delta\omega}{q_f-(-q_b)} \approx \frac{\Delta\omega}{2q_r};$$

i.e., V_g is also very small. It means that the chain of silver spheres in this regime (a narrow-band pulse comprising the frequency ω_r) is very efficient as a slow-wave line. It is easy to estimate that the wave whose wavelength is centered at 490 nm (it corresponds to ω_r in Fig. 1) and the spectral line width is 0.1 nm should possess the extremely small group velocity $V_g\approx 0.7\times 10^{-4}c$.

Finally, let us consider a possibility to excite the mode q_r using phase synchronism—e.g., by a parallel optical waveguide having wave number q_r at frequency ω_r. In this case the Poynting vector of the chain eigenmode should be nonzero and energy should propagate along the chain. However, such an excitation is possible at the only frequency (at which the dispersion curve of the exciting waveguide crosses that of the chain). Other frequency harmonics of the pulse propagating in the exciting waveguide have phase velocities that are different from the phase velocities of the chain harmonics. These frequencies are not supported by the chain. However, for a monochromatic wave $\omega=\omega_r$ there is no group velocity at all and nonzero energy flux is not forbidden. Naturally, excitation of a pulse with zero-frequency band is impossible, and the resonator-mode regime which is possible to obtain with a finite source can hardly be obtained with a phase synchronism due to the strong dispersion in the chain.

VI. POSSIBLE APPLICATION OF THE RESONATOR MODE

An evident application of the linear array supporting such a wave is a slow-wave line which should be very efficient. However, in the present paper we discuss another possible application of the chain of transversally polarized silver spheres. We mean its application for subwavelength imaging of a source, as discussed in the Introduction. Let us consider a structure formed by two such arrays (as shown in Fig. 4, on top). Assume, for example, that their parameters correspond to the dispersion plot shown in Fig. 1 and the source radiates a signal occupying the frequency range

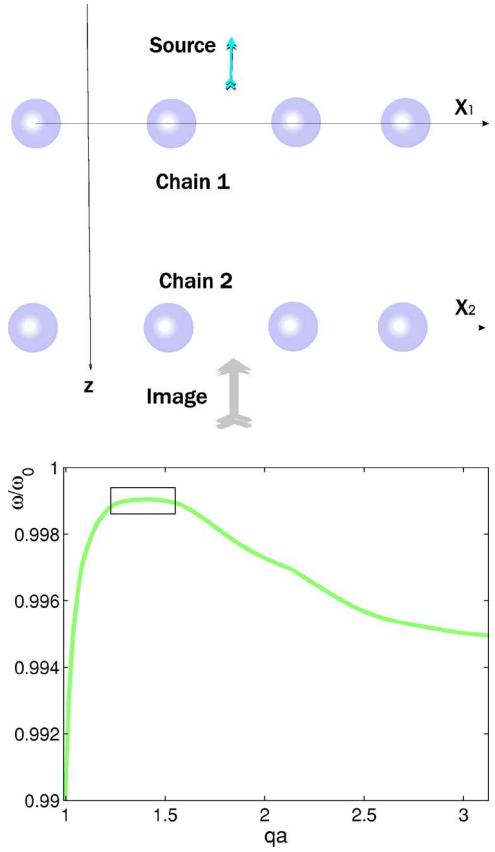

FIG. 4. (Color online) Top: a structure for near-field imaging across the chains. Bottom: the dispersion curve of a chain with $a=75$ nm, $d=30$ nm. There is a wide interval of q where the dispersion curve is practically flat (this interval is shown by the rectangle).

$0.998<\omega/\omega_0<0.999$. Consider the evanescent waves (with respect to the z axis) produced by the source. These waves are spatial harmonics with transverse wave numbers $|k_x|>0.999\omega_0/c$. These spatial harmonics will be supported by both chains within the range of $0.36\pi/a<|k_x|<0.6\pi/a$. In [2] the structure of two planar grids located in parallel planes X_1 and X_2 and supporting a surface wave with the wave vector **q** was considered. It was shown that if this surface wave in grid X_1 is excited by an evanescent wave attenuating along z (see Fig. 4), then in grid X_2 this wave will have an amplitude much higher than that in grid X_1. The corresponding evanescent wave will grow exponentially between X_1 and X_2. In Ref. [14] it was shown that in order to obtain this regime for the whole evanescent spatial spectrum of the source the grids X_1 and X_2 should be phase-conjugating surfaces. However, amplification of evanescent waves in a more or less narrow interval of spatial frequencies can be realized by linear systems. This fact was experimentally confirmed in [2]. A grid of antiparallel currents (in the microwave range) produced an evanescent wave with the wave vector **q** supported by a self-resonant sheet (formed by a planar array of meandered wire particles). This wave was strongly amplified across a pair of such sheets. Following the speculations of [2,14], the part of evanescent spatial spectrum supported at a given frequency by two identical chains will grow exponentially along z from chain 1 to chain 2 (see Fig. 4). Notice that such a structure operates with respect to the above-mentioned part of the evanescent spatial spectrum in the same way as Pendry's perfect lens [1] or a pair of perfect phase-conjugating surfaces [14] would operate with respect to the infinite evanescent spectrum.

At every frequency component ω of the signal radiated by a nonmonochromatic source the structure shown in Fig. 4, on top, will reproduce the amplitudes of these harmonics at a certain point (image) behind the axis X_2. Therefore a subwavelength image of the source located in front of chain X_1 will be obtained behind chain X_2. However, the variant of the dispersion curve plotted in Fig. 1 is not optimal for this purpose, and chains supporting waves with a wider range of wave numbers in the vicinity of the zero group velocity point can be designed. For such chains, a very-narrow-band signal will excite chain oscillations with a wider range of wave numbers, increasing the image resolution. The dispersion plot shown in Fig. 4 (bottom) demonstrates this possibility. Here, a more sparse chain ($d=30$ nm and $a=75$ nm) was chosen. The interval of wave numbers from $1.2/a$ to $1.6/a$ corresponds to the relative frequency band 10^{-4}.

The resolution can be further improved if more than one pair of chains is used and the images obtained with every pair of chains are unified. The signal of the same frequency in a chain with $d=25$ nm and $a=80$ nm resonantly excites waves with the wave numbers from $q_1=1.6/a$ to $q_2=2.1/a$. Likewise, a chain with $d=20$ nm and $a=85$ nm restores spatial harmonics from $q_1=2.0/a$ to $q_2=2.9/a$, practically at the same frequency. In this way one can form a near-field image produced by evanescent waves within the interval $q=1.2/a,\ldots,2.9/a$ using three superlenses, where every superlens contains two parallel chains of silver spheres with slightly different periods and different diameters. Finally, the wave-field image of the source can be obtained separately, and the source image including the contribution of evanescent waves can be restored numerically using the data obtained in these experiments.

VII. CONCLUSION

In this paper we have theoretically demonstrated a possibility to excite a standing wave in an infinite chain of plasmon particles (silver nanospheres) in the optical range. This standing wave (resonator mode) can be excited by a source positioned on the chain axis or near it and exists together with a traveling wave which has a much smaller amplitude.

We have studied the power flux spatial distribution at frequencies near the zero group velocity point ω_r. A time-harmonic source excites a dual-mode regime which has been analyzed in detail. At the frequency ω_r backward and forward waves (wave numbers q_r and $-q_r$) are excited with exactly the same amplitudes, and there is a standing wave in the chain. At frequencies $\omega\approx\omega_r$ the wave package is slowly traveling (a backward wave) and the power flux along the chain is nonzero (positive). If the source radiates a narrow-band pulse or a quasimonochromatic wave whose spectrum comprises the frequency ω_r, then the pulse with these frequencies excited in the chain represents a mixture of stand-

ing and traveling waves. The traveling-wave component is responsible for a nonzero but very small effective group velocity (this means effective excitation of a very slow wave) and to a very small power flux. The axial Poynting vector is negative on the chain axis and changes its sign at a certain distance ρ_0 from it, so that the total energy flux of the pulse turns out to be positive. The most part of the pulse energy propagating along the chain in the positive direction returns back inside a narrow spatial channel centered at the chain axis. This mechanism is responsible for a standing wave appearing in an infinite unbounded chain. Besides very efficient slow-wave lines these chains can be also used for obtaining subwavelength images.

ACKNOWLEDGMENTS

This work has been coordinated and partially funded by the "Metamorphose" Network of Excellence. Financial support of the Academy of Finland and TEKES through the Center-of-Excellence program is acknowledged. The authors would like to thank Dr. S.I. Maslovski and Professor I.S. Nefedov for useful discussions.

[1] J. B. Pendry, Phys. Rev. Lett. **85**, 3966 (2000).
[2] S. Maslovski, S. Tretyakov, and P. Alitalo, J. Appl. Phys. **96**, 1293 (2004).
[3] W. H. Weber and G. M. Ford, Phys. Rev. B **70**, 125429 (2004).
[4] S. A. Tretyakov, A. Viitanen, and C. R. Simovski, in Proceedings of the OSA International Topical Meeting: Nanophotonics for Information Systems, San Diego, CA, USA, 2005 (unpublished), p. 484.
[5] R. A. Shore and A. Yaghjian, Electron. Lett. **41**, 578 (2005).
[6] U. Kreibig, Z. Phys. **234**, 307 (1970).
[7] A. M. Belyantsev and A. V. Gaponov, Radio Eng. Electron. Phys. **8**, 980 (1964).
[8] V. N. Ivanov, N. P. Demchenko, I. S. Nefedov, R. A. Silin, and A. G. Schuchinsky, Izv. Vyssh. Uchebn. Zaved., Radiofiz. **32**, 764 (1989).
[9] I. V. Shadrivov, A. A. Sukhorukov, and Y. S. Kivshar, Phys. Rev. E **67**, 057602 (2003).
[10] A. C. Peacock and N. G. R. Broderick, Opt. Express **11**, 2502 (2003).
[11] D. Mori and T. Baba, Appl. Phys. Lett. **85**, 1101 (2004).
[12] A. Sanada, C. Caloz, and T. Itoh, IEEE Trans. Microwave Theory Tech. **52**, 1252 (2004).
[13] D. Sievenpiper, L. Zhang, R. Broas, N. G. Alexopoulos, and E. Yablonovitch, IEEE Trans. Microwave Theory Tech. **47**, 1252 (1999).
[14] S. Maslovski and S. Tretyakov, J. Appl. Phys. **94**, 4241 (2003).
[15] L. B. Felsen and N. Marcuvitz, *Radiation and Scattering of Waves* (IEEE Press, New York, 1994).